END
DATE
FILMED
8-8
DTI

MICROCOPY RESOLUTION TEST CHART

18 JUN 1982

COMPUTER DETECTION OF LOW CONTRAST TARGETS

RAUL G. MACHUCA, PHD
US ARMY WHITE SANDS MISSILE RANGE
WHITE SANDS MISSILE RANGE, NEW MEXICO 88002

Introduction. At White Sands Missile Range we are interested in detecting manmade objects (targets) usually against a natural background such as the sky or a mountain. A widely used method of detecting a target is to find the edges in a picture using some operator whose value is high when there are many changes in gray levels. An object which contrasts with the background because of step and ramp edges gives rise to high values of the edge detector. After the detection of the step and ramp edge points in a scene, the problem of detecting a target is reduced to that of determining which of the points classified as edges belong to the target. If the target is the object of greatest contrast then its location can be found by simply thresholding for the highest value of the edge detector. However, if the target is not the object of highest contrast other methods must be used to detect a target in a scene. Thus, we must use properties of the target that are not shared by other edge points in a scene. The targets that we track, planes and rockets, have as one of their main geometric features several points of very high curvature. Thus, to detect edges which belong to a target a reasonable procedure would be to look for edge points which come from objects which have high curvature. Another property which makes manmade objects different from natural objects is the strong interior edges (extremal edges) which are present. This suggests that another procedure for detecting objects such as planes and rockets is to measure in some way the extremal edges present in a scene and to look for the target amongst those points of higher values. It may be possible that the information present in the gray level picture does not have any significant difference in gray level between the target and the background but the target and the background may be of different colors. In this case, we must look a the color information and extract the edges from the color data before we begin to look for a target. The problems of finding extremal edges, finding curvatures along the boundary of objects, and detecting color edges, at first sight appear unrelated. The formulation of these problems in the framework of vector fields and the application of

82 07 19 245

this theoretical model to data both from the range and from the laboratory are the subjects of this paper.

The paper is divided into three parts. In the first section we discuss extremal edges and their detection, section 2 discusses curvature and its measure and section 3 formulates the detection of color edges in vector field language and uses the theoretical results of sections 1 and 2 to detect color edges. Each section follows the same paradigm, namely:

1. The problems is formulated as a problem in the theory of vector fields.

2. The detection of a particular property is formulated as the computation of an integral over a vector field, AND

3. The theoretical results are applied to data obtained from the field or in the lab.

An outline of the mathematical methods are ~~mostly~~ contained ~~in section 1~~ and are based on classical vector analysis. Details of the mathematics used appear ~~in [8] and [9]~~ for supporting material on differential geometry, see for example [1] or [2]. What we call the rotation degree of a vector field is also called the topological degree of the corresponding mapping from the unit circle to itself. Two books treating topological degree theory are [3] and [4].

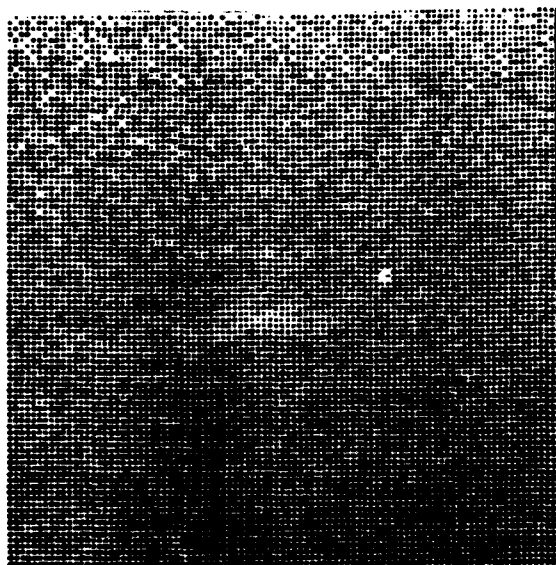## Section I. VECTOR FIELDS AND EXTREMAL EDGES

The two planes of figure 1 are typical of the tracking situations that occur at WSMR. To set these we started with the original video frames and digitized the analog signal at the rate of 512 points per line. The value assigned to each point is between 0 and 255 and is proportional to the strength to the analog signal. In these two pictures, that are of very low contrast, we have been able to segment the target by finding the extremal edges arising from the shape of the fuselage and wings. In terms of a function of two variables an extremal edge is a connected set of extrema very similar to the top points of a roof. The classical development of extrema via partial derivatives does not give a method for finding these extrema. The standard treatment of critical points looks at the quadratic form $f_{11}f_{22} - f_{12}^2$ and at f_{11} using the Hessian

$$Hf = \begin{bmatrix} D_{11}f & D_{12}f \\ D_{21}f & D_{22}f \end{bmatrix}$$

Justification

By

Distribution/
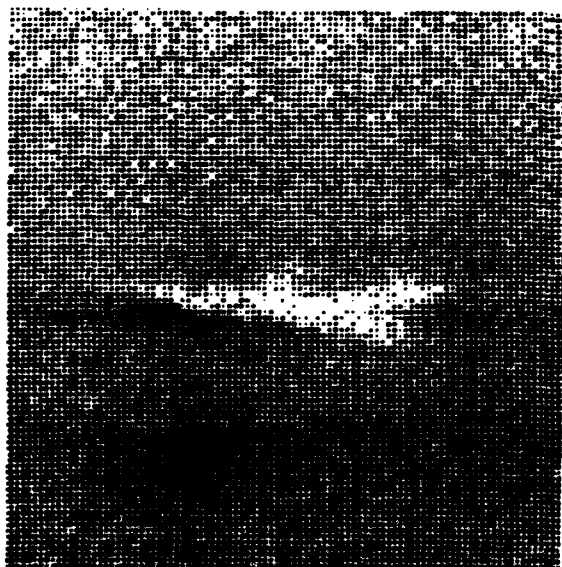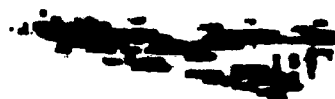
Availability Codes

Dist	Avail and/or Special
A	

Figure 1. (a) (c) Two planes as seen through a telescope. (b) (d)
extremal edges of (a) and (c) segment the planes from the
background.

the conditions for an extrema are:

max: determinant (Hf) >0 and $f_{11}<0$
min: determinant (Hf) >0 and $f_{11}>0$
non-extrema: determinant (Hf) <0
cannot say: determinant (Hf) = 0

An example of a function about which nothing can be said from this test is $Z = X^4 + Y^4$. It has a Hessian which vanishes at 0 and thus from this test no conclusion can be made about the type of critical point at (0, 0) even though it is obviously a minimum. The gradient field shows that the function is increasing at every direction away from (0, 0) and so the information as to the nature of the extrema is in the gradient field.

We can extract this information from the vector field by calculating the integral for $z=x^4 + Y^4$

$$\eta = \frac{1}{2\pi} \int_\gamma d\theta \frac{1}{2\pi} \int_\gamma K = 1$$

where

$$(a) \quad K(\bar{x}) = \frac{Hf(\tilde{x}, \tilde{\triangledown} f(\tilde{x}))}{|f(\bar{x})|^2}$$

$$(b) \quad Hf(\tilde{x}, \tilde{\triangledown} f(\tilde{x})) = \begin{bmatrix} D_{11}f & D_{12}f \\ D_{21} & D_{22}f \end{bmatrix} \begin{pmatrix} -D_2 f \\ D_1 f \end{pmatrix}$$

$$(c) \quad \tilde{\triangledown} f(\bar{x}) = (-D_2 f, D_1 f)$$

and $d\theta$ is the $d\theta$ of (figure 2).
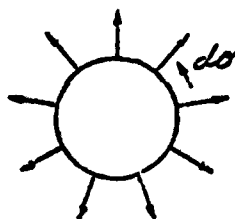

Figure 2.   A portion of a vector field.

The fact that Z is an extrema at (0,0) is reflected by its nonzero value of η. But we are mainly interested in detecting extrema which are not isolated as in the case $f=x^2$. This function has the line x=0 as the set of its extrema. If we look at the Hessian it gives no information which can be used to detect the extremal set: As before we must look at the gradient field to find the extrema. The gradient field of the function as before reveals the behavior of the function at x=0, namely it is increasing as we move away from x=0, thus there is an extremal edge along the line x=0.
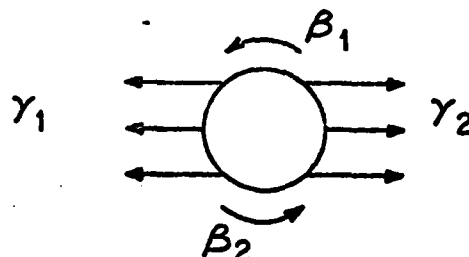
$$\beta_1$$

$$\gamma_1 \qquad \gamma_2$$

$$\beta_2$$

Figure 3. A small neighborhood of the gradient field for the function $z=x^2$.

Because of the ambiguous dθ at β^1 and β^2 (figure 3) the analytical detector of extrema edge points becomes somewhat complicated. The analogy of isolated extrema is followed and we define the detector as an integral along the places where it can be defined and where there is an ambiguity we take d$\theta=\pi$. Using the quantities defined at (a) and (b) the analytical detector is

$$\eta = \int_{\gamma_1} K dr \quad + \int_{\gamma_2} K dr + \beta_1 + \beta_2$$

This gives a function which is equal to zero at nonextremal edges and 1 at extremal edges.

Once we have identified the external edges we want to distinguish between weak and strong extremal edges. In the one dimensional case (figure 4) the quantity $M(e) = |f'(a)| + |f'(b)|$ will distinguish between sharply sloped roofs and weakly sloped roofs. The two dimensional analogue of this quantity is $\int_\gamma |f\nabla|$.

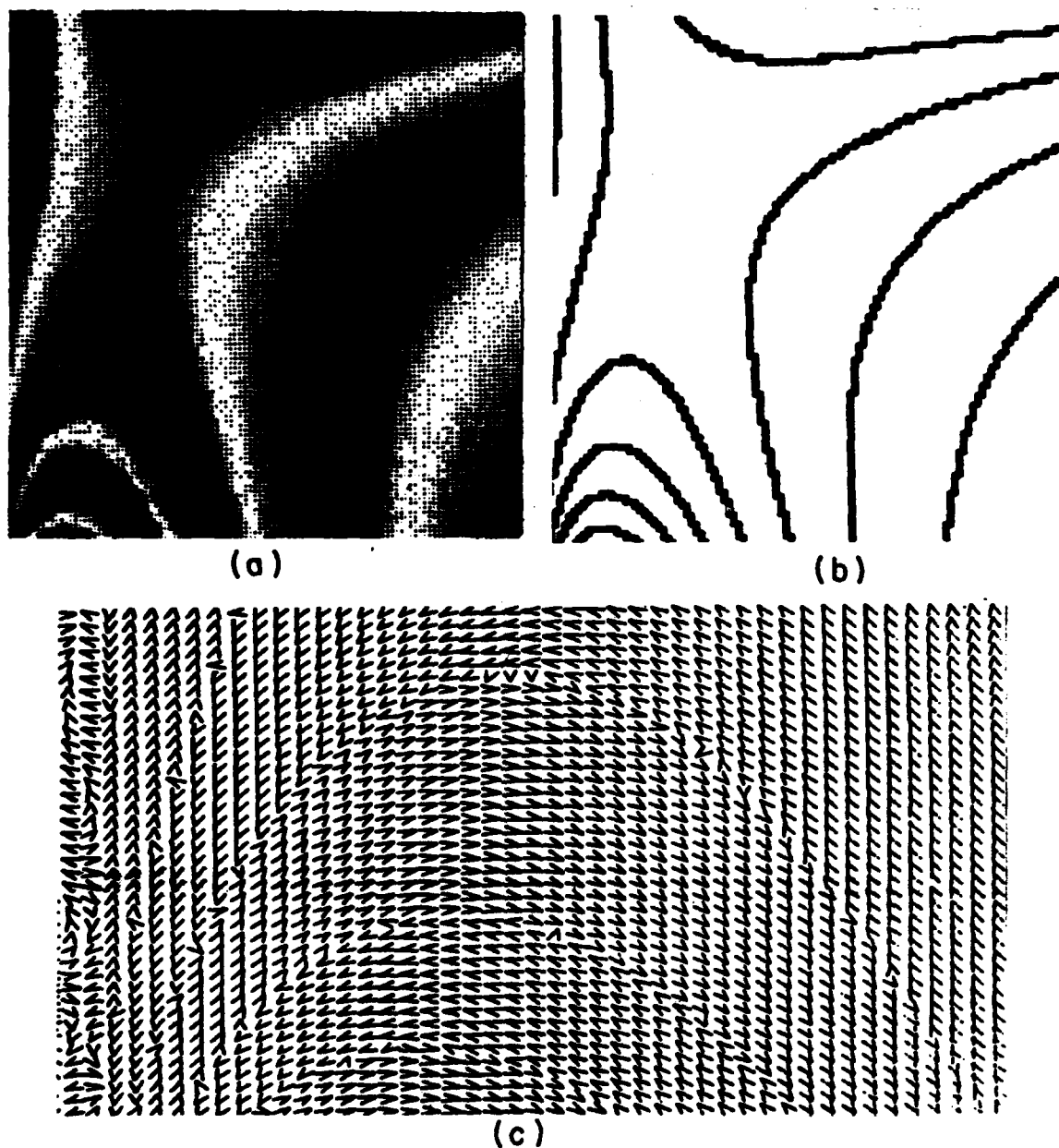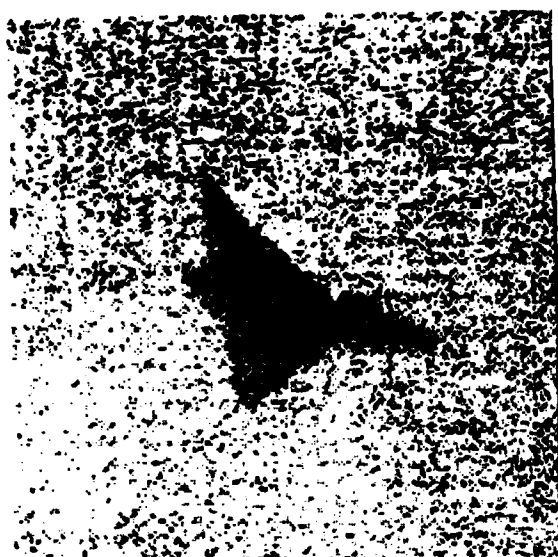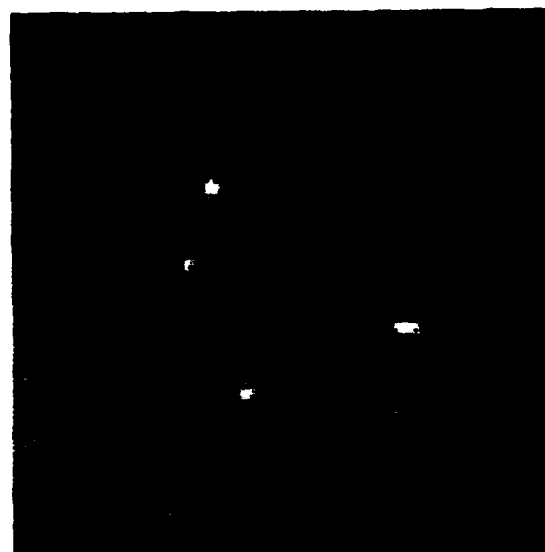Figure 4. Weak and strong extremal edges.

Figure 5. (a) Computer generated example, (b) edge points detected,
and (c) partial gradient field of (a) rotated 90 degrees.
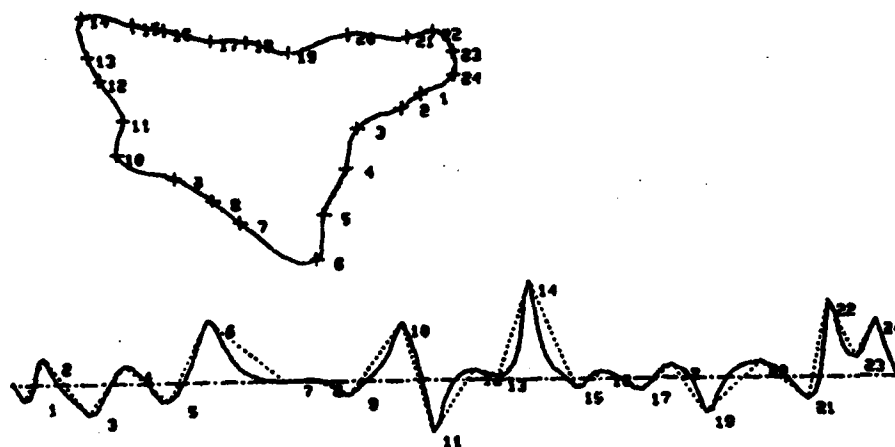
(a)

(b)

(c)

Figure 6.   (a) Digitized video frame of an F102, (b) areas of high
            curvature, and (c) contour of (a) and its curvature.

The computer application of these methods is done by first approximating the partials in a 3x3 neighborhood of a point and from this computing the quantities $d\theta$ and ∇f. A new file is created which contains $\int_\gamma |\nabla f|$ when $\eta=1$ and 0 when $\eta = 0$.

In figure 5 we have several extremal edges of the type $z=x^2$ and $z=-x^2$. The darkest parts are like the extreme points $z=+x^2$ while the brightest points are like the extrema $z=-x^2$. The edge points exhibited in figure 5 have been found using the procedure described above. Figure 1 contains pictures of a plane taken through long distance optics. There is very little contrast in both pictures between the plane and the background. However, the extremal edges which result from the wings and the fuselage are very easily detected by the methods described above.

Section II. CURVATURE

This concept of studying the gradient field to find properties of a scene can be used to find other features of a target. For example in figure 6, the points of the original in which the contour has high curvature have been found by looking at the gradient vector field.

The analytical tools used to detect curvature are the same as those used in detecting extremal edges. With the definitions the same as (a), (b), and (c) above, the pointwise curvature can be computed from the Hessian and the gradient and is given by the formula

$$W(\bar{x}) = - < \frac{Hf(\bar{x}, \tilde{\nabla}f(\bar{x}), \tilde{\nabla}f(\bar{x}))>}{|\nabla f|^3}$$

Because of the amount of noise present in these scenes a better quantity to compute is the average curvature:

$$A^* (K,\beta) = \frac{1}{\beta} \int \beta W \, dr$$

To see that the quantity is a measure of curvature we look at the function $f(x,y) = x^2 + y^2$ and compute A^* for this function. If A^* is computed over a small circle centered at n as in figure 7,
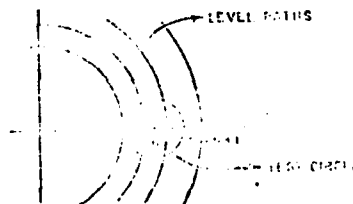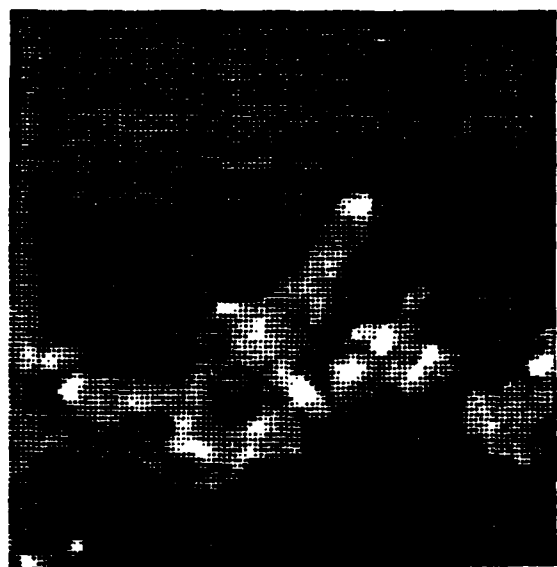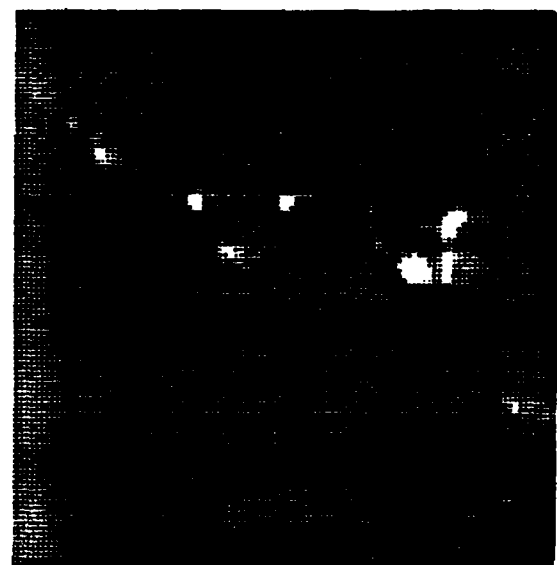

Figure 7. Contour lines and test circle.

Figure 8.   Missile (a) and plane (c) with area of high curvature
(b) and (d).

then if A* is a good measure of curvature it should be small when n is large and large when n is small. Using polar coordinates the pointwise curvature is 1/r and with the circles parametrized by $(n,0) + e^{it}$, A* becomes the integral

$$\int_{-\Pi}^{\Pi} \frac{dt}{(n^2 + 1 + 2n \cos t)^{1/2}}$$

and this integral is a maximum for n=1 and decreases as n increases, exactly what a good measure of curvature should do. Figure 8 contains two scenes obtained from range missions. Figure 8 (a) is a rocket at takeoff. The nose of the rocket has been identified as one of the points of high curvature and is the brightest point of (b) closest to the top. The points of high curvature generated by the plume are also indicated. In figure 8 (c) there is a plane flying by a mountain. The points of high curvature at the nose, wing, and tail have been detected. There are also some others from the mountain edge. Thus, the gradient field reflects many properties of the original scene. We can also look at other vector fields generated by scenes and find other properties such as color edges.

Section III. COLOR EDGES

We are mainly interested in the analysis of color data in the case where there is no gray level difference between the target and the background, i.e., in the cases where the above methods fail. That is we are looking for a method for finding edges in the case where the target cannot be separated from the background by looking at the luminance component of a scene but can be detected by using the chrominance information. A widely used color representation that breaks up a color into luminance and chrominance information is the (Y,I,Q) color representation of standard video. In this representation Y is the luminance component, which we ignore since our principal assumption is that the target and background are similar in luminance. Thus we must look at the I and Q components to detect the target from the background, and in particular we are interested in edges caused by differences in hue between target and background.

For any color (Y,I,Q) the vector v = (I,Q) has the property that the angle it makes with the I - axis, $\Theta(v)$, specifies its hue (see figure 9) while its absolute value gives the saturation.
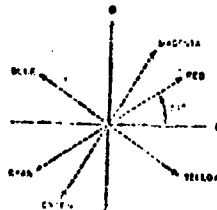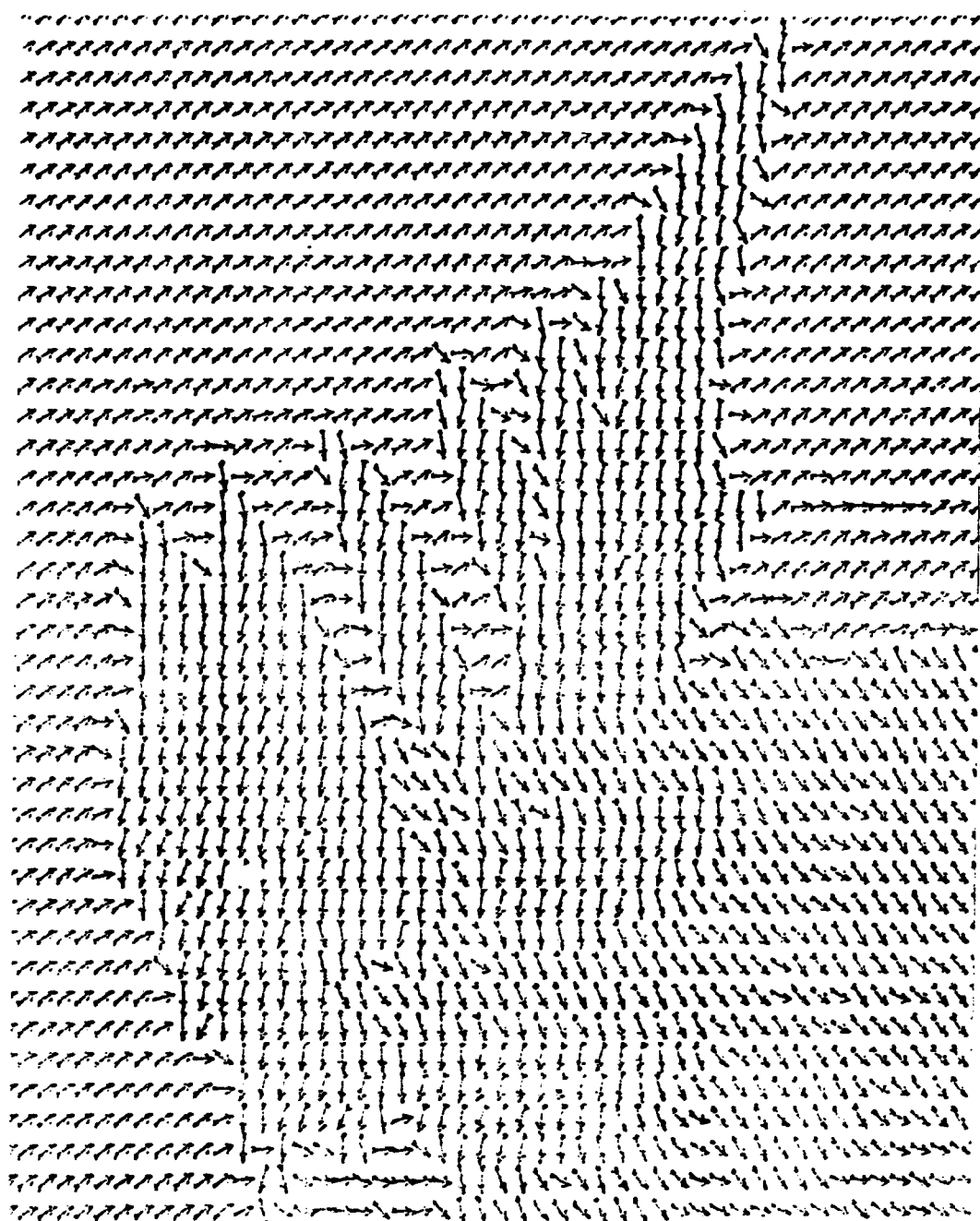

Figure 9. The I, Q Coordinate System

Figure 10. The (1,0) vector field in the neighborhood of a leaf.

ie assume that the saturation is the same for every color of an image
s is the case for the scenes we study) then the color information
lable to detect the target is all contained in θ(v). In order to
ct the edges from this component, it is useful to consider the vector
d T = v/|v| and use the vector field formulation of section I to
ct edges due to hue.

An example of a vector field T so generated appears in figure 10. A
.ion of the vector field on a test circle, selected from near the
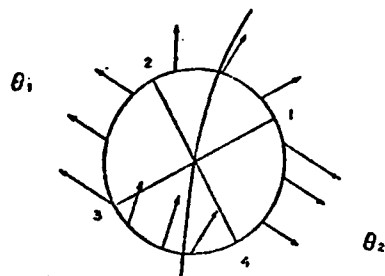er of figure 10 is shown in figure 11.

Figure 11. A portion of a color edge.

figure 11, we detect an edge between the two colors, θ_1(blue) and
ellow), simply because the vectors point in opposite directions. Note
T rotates counterclockwise from 1 to 2 to 3, clockwise from 3 to 4 to
There are convexity changes at approximately "1" and "3". If the

le γ is parametrized on [0,1] by $\gamma(t) = e^{2\pi it}$, then the argument

tion θ(t) is simply θ = Arg(v) at the point $e^{i2\pi t}$ on the circle:

$$T(t) = (\cos(\theta(t)), \sin(\theta(t))).$$

early, because if we use the integral as the color edge detector,

$$(ii) \quad \int_0^1 |\theta(t)|\,dt = \int_\gamma |d\theta|$$

ignore the change in convexity and measure net rotation.   From
re 11 it is clear that

$$(iii) \quad \int_\gamma |d\theta| = 2\,|\theta_1 - \theta_2|\;.$$

Figure 12. The R, G, B components of "girl picture" (a), (b) (c) and the hue edgepoints (d).

The integral $\int_\gamma d\theta$ in (ii) can be interpreted as the average curvature of the vector field T; e.g., as in (iii) for the curve γ. Hence, measuring net rotation corresponds to measuring the average curvature of T on γ. We have found $\int_\gamma d\theta$ to be a good color edge detector. In fact the vector field shown in figure 10 is generated by the leaf in the R,G,B components shown in figure 12 a-b-c. The result of the average curvature method $- \int_\gamma d\theta -$ is shown in figure 12.

An alternate approach to detecting color edges would be to follow the classical development for gray level edges. That is compute abs(grad(R)), abs(grad(G)), and abs(grad(B)) and combine these in some way to find the color edges. This process requires that two convolutions take place for each of the gradients (one for each partial derivative), and after the gradients are computed there remains the problem of how to combine them into one output.

The edge detection method described in this section is particularly provocative because of its implications with regard to hardware implementations of color edge detectors. The phase of the (I,Q) vector is easily available from analog hardware and so the data input to this algorithm is available in real time. The integration that takes place for the edge detection is a type of "convolution" easily performed by state-of-the-art real time hardware. Thus, with this method an implementation can be constructed with components that are practically available off the shelf, and such a machine is being built at White Sands Missile Range.

Conclusion. We have shown that a variety of image processing problems can be stated in terms of vector field problems and that quantities easily calculated in real time over the associated vector fields can be used to detect image features. Extremal edges can be found by computing the rotation number of a curve α via a simple process. Points of high average curvature are found directly from the vector field, without approximate surfaces or statistics. It was shown that the detection of hue edges could be done by computing the rotation associated with the vector field (I,Q), a number that can easily be computed in real time by existing hardware components.

REFERENCES

1. Klingenberg, Wilhelm, A Course in Differential Geometry, Springer-Verlag, 1978.

2. Spivak, Michael, Differential Geometry, vol. II, 1970.

3. Milnor, John, Topology From the Differentiable Viewpoint, University of Virginia Press, 1965.

4. Lloyd N. G., Degree Theory, Cambridge University Press, 1978.

5. Machuca, R. and Gilbert, A., "Finding Edges in Noisy Scenes", IEEE Transactions on Pattern Analysis and Machine Intelligence, vol. 3, No. 1, pp. 102-111, January 1981.

6. Barnard, S. C., and Thomson, W. B., "Disparity Analysis of Images", IEEE Transactions on Pattern Analysis and Machine Intelligence, vol. 2, No. 4, pp. 333-340, July 1980.

7. Kitchen, L., and Rosenfeld, A., "Gray Level Corner Detection", TR-887, Computer Sciences Center, University of Maryland, College Park, MD, April 1980.

8. Machuca, R., and Phillips, K., "Applications of Vector Field Theory to Extremal Edge Detection", Proceedings of the IEEE SOCON, Orlando, FL, March 1982.

9. Machuca, R., and Phillips, K., "Applications of Vector Fields to Image Processing", To appear in IEEE Transactions on Pattern Analysis and Machine Intelligence.